Journal of Molecular Neuroscience (2018) 65:60–73
https://doi.org/10.1007/s12031-018-1070-x

# Mesenchymal Stem Cells Form 3D Clusters Following Intraventricular Transplantation

Nicole Jungwirth[1,2] · Laura Salinas Tejedor[2,3] · Wen Jin[1,2] · Viktoria Gudi[2,3] · Thomas Skripuletz[3] · Veronika Maria Stein[4] · Andrea Tipold[2,4] · Andrea Hoffmann[5] · Martin Stangel[2,3] · Wolfgang Baumgärtner[1,2] · Florian Hansmann[1,2]

Received: 8 March 2018 / Accepted: 19 April 2018 / Published online: 28 April 2018


## Abstract

Mesenchymal stem cells (MSCs) are regarded as an immune privileged cell type with numerous regeneration-promoting effects. The in vivo behavior of MSC and underlying mechanisms leading to their regenerative effects are largely unknown. The aims of this study were to comparatively investigate the in vivo behavior of canine (cMSC), human (hMSC), and murine MSC (mMSC) following intra-cerebroventricular transplantation. At 7 days post transplantation (dpt), clusters of cMSC, hMSC, and mMSC were detected within the ventricular system. At 49 dpt, cMSC-transplanted mice showed clusters mostly consisting of extracellular matrix lacking transplanted MSC. Similarly, hMSC-transplanted mice lacked MSC clusters at 49 dpt. Xenogeneic MSC transplantation was associated with a local T lymphocyte-dominated immune reaction at both time points. Interestingly, no associated inflammation was observed following syngeneic mMSC transplantation. In conclusion, transplanted MSC formed intraventricular cell clusters and exhibited a short life span in vivo. Xenogeneically in contrast to syngeneically transplanted MSC triggered a T cell-mediated graft rejection indicating that MSCs are not as immune privileged as previously assumed. However, MSC may mediate their effects by a "hit and run" mechanism and future studies will show whether syngeneically or xenogeneically transplanted MSCs exert better therapeutic effects in animals with CNS disease.

**Keywords** Mesenchymal stem cells · Canine mesenchymal stem cells · Human mesenchymal stem cells · Cell clusters · CD44 · Host versus graft reaction

## Introduction

Mesenchymal stem cells (MSCs) can be isolated from a large variety of different tissues including bone marrow and adipose tissue (Barry and Murphy 2004; Singer and Caplan 2011). MSCs are characterized by their adherence to plastic, an expression of a specific marker panel, and their ability to differentiate along the mesodermal lineage (Dominici et al. 2006; Edamura et al. 2012; Friedenstein et al. 1966; Hernigou 2015; Singer and Caplan 2011; Woodbury et al. 2000). Within the last years, MSCs were frequently applied as the second- or third-line regenerative approach in a variety of inflammatory, degenerative, and demyelinating diseases. Therapeutic application of MSC was promoted by various in vitro and in vivo studies demonstrating homing of MSC towards damaged tissue sites as well as their immunomodulatory and regenerative properties (Barry and Murphy 2004; Bernardo and Fibbe 2013; Karp and Leng Teo 2009; Le Blanc and Mougiakakos 2012; Uccelli et al. 2008). Furthermore, more than 500 studies are listed in the database at www.ClinicalTrials.gov, testing the therapeutic efficiency of MSC in human medicine. Recently, interest in dogs significantly increased since the dog serves as a large animal model for spontaneously occurring inflammatory and degenerative diseases of the

✉ Wolfgang Baumgärtner
wolfgang.baumgaertner@tiho–hannover.de

[1] Department of Pathology, University of Veterinary Medicine Hannover, Bünteweg 17, 30559 Hanover, Germany

[2] Center for Systems Neuroscience, Hannover, Germany

[3] Clinical Neuroimmunology and Neurochemistry, Department of Neurology, Hannover Medical School, Hannover, Germany

[4] Department of Small Animal Medicine and Surgery, University of Veterinary Medicine Hannover, Hannover, Germany

[5] Department of Orthopaedic Surgery, Hannover Medical School, Hannover, Germany

central nervous system (CNS) such as spinal cord trauma due to intervertebral disc herniation (Jeffery et al. 2006; Spitzbarth et al. 2012). Many studies investigated the efficacy of canine MSC (cMSC) for the treatment of canine musculoskeletal system diseases but only few studies focused on MSC for the treatment of CNS diseases (de Bakker et al. 2013; Fortier and Travis 2011; Harding et al. 2013; Jung et al. 2009; Whitworth and Banks 2014). This study comparatively investigated the capability of cMSC, human MSC (hMSC), and murine MSC (mMSC) with regard to proliferation, differentiation, functional integration, and their interaction with the immune system following intraventricular transplantation in immunocompetent mice.

## Material and Methods

### Isolation and Cultivation of MSC

cMSCs were isolated from abdominal adipose tissue of a healthy, 1-year-old, male beagle dog as previously described with minor modifications (Martinello et al. 2011). Abdominal adipose tissue was divided into small pieces, cleaned from large blood vessels and fibers, mechanically minced, and digested with 10 mg/ml collagenase D (Roche, Basel, Switzerland) for 30 min under constantly stirring at 37 °C. Subsequently, cell suspension was filtered through a 100-μm cell strainer (BD Bioscience, Heidelberg, Germany) and centrifuged at 1400*g* for 20 min followed by a washing step in phosphate-buffered saline (PBS) and a second centrifugation step at 1600*g* for 10 min. Cells were seeded into T25 flasks (VWR, Darmstadt, Germany) with low-glucose Dulbecco's modified Eagle's medium (DMEM-LG; Biochrom, Berlin, Germany) containing 11.6% fetal bovine serum (FBS; HyClone, Thermo Fisher Scientific, Schwerte, Germany), HEPES 1 M (Biochrom, Berlin, Germany), 1% penicillin/streptomycin (PAA, Marburg, Germany), and 0.002% human recombinant fibroblast growth factor 2 (FGF-2; Preprotech, Hamburg, Germany) at a concentration of $1.3 \times 10^5$ cells/ml. Cells were incubated at standard conditions (37 °C, 5% $CO_2$) and medium was changed every third day until 80% confluency. Cells were dissociated with Trypsin-EDTA (PAA, Marburg, Germany) and further passaged until passage 2 (P2) and cryopreserved. Cryopreservation was performed with 10% dimethyl sulfoxide (DMSO; Hybri-Max; Sigma-Aldrich, Seelze, Germany), 25% FBS (HyClone, Thermo Fisher Scientific, Schwerte, Germany), and 65% DMEM-LG (Biochrom, Berlin, Germany). Thawed cells from P2 were used for in vitro differentiation, flow cytometry, and transplantation experiments.

Human bone marrow-derived mesenchymal stem cells (hMSCs) were isolated from a healthy, female donor. The bone marrow aspirate was mixed with three volumes of PBS (without $Ca^{2+}$ and $Mg^{2+}$) and filtered (100 μm) to remove tissue debris. The resulting suspension was carefully layered onto one volume Biocoll ($\rho = 1.077$ g/ml) and centrifuged for 30 min at 500×*g* without brake in conical centrifuge tubes (50 ml volume). The mononuclear cells located at the interface of the density gradient were harvested using a Pasteur pipette, washed once in PBS, resuspended in MSC expansion medium, and seeded in cell culture flasks (75 $cm^2$ culture area per 50 ml gradient). The MSC expansion medium consisted of DMEM-LG (1 g/l glucose, Biochrom, Berlin, Germany) supplemented with 10% (*v*/*v*) fetal bovine serum (not heat-inactivated, HyClone, Thermo Fisher Scientific, Schwerte, Germany), 25 mM HEPES (Biochrom, Berlin, Germany), 1% penicillin/streptomycin (Biochrom, Berlin, Germany), and 2 ng/ml human recombinant FGF-2 (from *Escherichia coli*, PeproTech, Hamburg, Germany). The cells were cultured at 37 °C with 5% $CO_2$ at 85% humidity. Twenty-four hours later, the medium was removed and replaced by fresh MSC expansion medium, and subsequent media changes were performed every 3–4 days. The cells were passaged at a density of around 70% by the use of 0.05%/0.02% (*w*/*v*) Trypsin-EDTA solution (Biochrom) and seeded at a density of 2000 cells/$cm^2$.

Murine MSCs (mMSCs; Cyagen Bioscience, Santa Clara, USA) originating from bone marrow of C57BL/6N mice expressing red fluorescent protein (RFP) were cultured according to the manufacturer's instructions (Salinas Tejedor et al. 2015). Briefly, mMSCs were seeded into T75 flasks and cultivated in OriCell™ Mouse Mesenchymal Stem Cell Growth Medium (Cyagen Bioscience, Santa Clara, USA) at standard culture conditions. Medium was changed every third day until 80–90% confluency. For dissociation, mMSCs were rinsed two times with PBS (without $Ca^{2+}$ and $Mg^{2+}$, Gibco, Karlsruhe, Germany) followed by incubation with 0.25% Trypsin and 0.04% EDTA. Trypsin reaction was stopped using OriCell™-Medium under light microscopic control.

### In Vitro Characterization of MSC

cMSCs were characterized using flow cytometry and in vitro differentiation along the adipogenic, osteogenic, and chondrogenic lineages as described (de Bakker et al. 2013; Guercio et al. 2013; Han et al. 2012; Reich et al. 2012; Screven et al. 2014; Stein et al. 2004; Vieira et al. 2010). Adipogenic differentiation of MSC was performed according to Guercio et al. (2013) with minor modifications. Briefly, cMSCs were plated at a density of $1 \times 10^5$ cells/well in a 24-well plate (Nunc, Thermo Fisher Scientific, Schwerte, Germany). Two days post seeding, medium was changed and cells were incubated in Complete MesenCult® Adipogenic Medium (STEMCELL, Grenoble, France). Half-medium volume was changed every second day, and after 10 days, cells were fixed in formalin and stained with Oil

red O for the detection of lipid droplets. For osteogenic differentiation, cMSCs were seeded at a density of $1 \times 10^5$ cells/well in a 24-well plate (Nunc, Thermo Fisher Scientific, Schwerte, Germany) and incubated in DMEM-LG containing 10 M β-glycerophosphate (Sigma-Aldrich, Seelze, Germany), 0.1 μM dexamethasone (Sigma-Aldrich, Seelze, Germany), 20% FBS (HyClone, Thermo Fisher Scientific, Schwerte, Germany), 1.5% penicillin/streptomycin (PAA, Magdeburg, Germany), and 0.2 M ascorbate-2-phosphate (Sigma-Aldrich, Seelze, Germany) as previously described by Han et al. (2012). Medium was changed every third day, and after 14 days, cells were fixed in formalin and stained with von Kossa as well as Alizarin red S for the detection of calcium deposits. Chondrogenic differentiation was performed according to Reich et al. (2012) with minor modifications. Briefly, cMSCs were placed at a density of $2.5 \times 10^5$ into a falcon tube with DMEM-LG and centrifuged at 100*g* for 5 min. The cell pellet was incubated under standard culture conditions overnight. Medium was changed and cells were incubated in DMEM-LG containing 1% FBS, 1% penicillin/streptomycin, 0.05% of a combination of insulin, transferrin, selenium, linoleic acid, and bovine serum albumin (ITS+™ Premix; BD Bioscience, Heidelberg, Germany), 50 μM ascorbic acid (Sigma-Aldrich, Seelze, Germany), 100 nM dexamethasone (Sigma-Aldrich, Seelze, Germany), and 10 ng/ml TGF-β1 (Sigma-Aldrich, Seelze, Germany). Medium was changed every third day, and after 14 days, cells were fixed in formalin and stained with Alcian blue.

Flow cytometry of cMSC was performed using FACSCalibur™ (Becton and Dickinson, Heidelberg, Germany) and Cell-Quest® software (BD Biosciences, Heidelberg, Germany) as previously described (Stein et al. 2004). For each sample, 5000 to 10,000 live gated events were analyzed. cMSCs were adjusted to a concentration of $2 \times 10^5$ cells/tube in MIF buffer (PBS, 1% BSA and 0.1% NaN3 10%). Blocking was performed using human IgG Fc-blocking solution (1:8; Human TrueStrain FcX, BioLegend, Biozol, Eching, Germany). Primary antibodies as listed in Table 1 were applied to the cell suspension for 30 min at 4 °C. Unconjugated antibodies were detected using the following secondary antibodies peridinin chlorophyll protein complex (PerCP)-conjugated goat anti-rat IgG (1:50; Dianova, Hamburg, Germany), R-phycoerythrin (RPE)-conjugated goat anti-mouse IgG (1:100; Dianova, Hamburg, Germany), or RPE polyclonal rabbit anti-rat IgG (1:100; AbDSerotec, Star20A, Puchheim, Germany). Species-specific isotype controls diluted according to the immunoglobulin concentration of the respective primary antibody served as negative controls.

As detailed by Nessler et al. (2013), hMSCs were phenotypically characterized by flow cytometry using antibodies targeting CD49d, CD73, CD90, and CD105 (Table 1) before transplantation.

mMSCs were phenotypically characterized by flow cytometric analysis using antibodies targeting CD44 and Sca-1 (Table 1) before transplantation as previously described (Nessler et al. 2013; Salinas Tejedor et al. 2015).

## Study Design

Experiments were performed using 5-week-old, immunocompetent, female SJL/JCrHsd as well as C57BL/6N

**Table 1** Antibodies, suppliers, catalog numbers, sources, clonalities, labeling, and dilution for flow cytometric analysis

| Primary antibody | Supplier | Catalog number/RRID | Source and clonality | Labeling | Dilution |
|---|---|---|---|---|---|
| CD29 | Biorbyt[a] | orb44012/AB_10994112 | Mouse MC | Dylight647 | 1:5 |
| CD44 | AbDSerotec[b] | MCA1041GA/AB_2074682 | Rat MC | – | 1:100 |
| CD44 | BioLegend[c] | 103032/AB_2076204 | Rat MC | PerCP/Cy5.5 | 1:100 |
| CD45 | AbDSerotec[b] | MCA104B/AB_322956 | Rat MC | Biotin | 1:5 |
| CD49d | BioLegend[c] | 304313/AB_10642817 | Mouse MC | PE/Cy7 | 1:100 |
| CD73 | BioLegend[c] | 344003/AB_1877224 | Mouse MC | PE | 1:100 |
| CD90 (Thy-1) | BioLegend[c] | 328113/AB_893440 | Mouse MC | APC | 1:100 |
| CD90 (Thy-1) | e-Bioscience[d] | 17-5900/AB_10732355 | Rat MC | APC | 1:20 |
| CD105 | BioLegend[c] | 323217/AB_10895769 | Mouse MC | PE/Cy7 | 1:100 |
| MHC I (H58A) | Monoclonal Antibody Center[e] | CT-BOV2001/AB_2722788 | Mouse MC | – | 1:100 |
| Sca-1 | BioLegend[c] | 108111/AB_313348 | Rat MC | APC | 1:100 |

*APC* allophycocyanin, *CD* cluster of differentiation, *MC* monoclonal, *PC* polyclonal, *PE* R-phycoerythrin, *PerCP* peridinin-chlorophyll-protein

[a] Cambridge, UK

[b] Puchheim, Germany

[c] San Diego, USA

[d] Frankfurt, Germany

[e] Washington, USA

mice (Harlan, Horst, Netherlands). Mice were housed in isolated ventilated cages (Tecniplast, Hohenpeißenberg, Germany) in a controlled environment (22.5 ± 1 °C, 55 ± 5% relative humidity, 12-h light/dark cycle, 74 changes of air per hour), fed ad libitum with a standard rodent diet (R/M-H; Ssniff Spezialdiäten GmbH, Soest, Germany), and had free access to tap water. For xenogeneic transplantation, 24 SJL mice were randomly distributed into groups ($n = 6$ animals per group) receiving an intraventricular transplantation of either cMSC or hMSC. For syngeneic transplantation, C57BL6/N mice ($n = 8$ animals) received an intraventricular transplantation of mMSC. Perfusion and necropsy was performed at 7 dpt (all groups) and 49 dpt (cMSC- and hMSC-transplanted animals) as described (Hansmann et al. 2012).

## MSC Transplantation

Anesthesia was induced by an intra-peritoneal injection of medetomidine (0.5 mg/kg, Domitor®, Pfizer, Berlin, Deutschland) and ketamine (100 mg/kg, Ketamin®, WDT, Garbsen, Germany) as described (Hansmann et al. 2012; Herder et al. 2012). Analgesia was achieved by intraoperative tramadol (15 mg/kg Tramadol Ratiopharm®, Ratiopharm, Ulm, Germany) and carprofen (4 mg/kg, Rimadyl®, Pfizer, Berlin, Germany) injection. Stereotaxic injections were performed using a small animal stereotaxic instrument (TSE Systems, Bad Homburg, Germany). For injections, a 10-µl syringe (Hamilton, Bonaduz, Switzerland) with a 60-µm (inner diameter) glass capillary (Drummond Microcaps®, Sigma-Aldrich, Seelze, Germany) previously stretched with a puller system (Narishige, London, Great Britain) was used. A total of $1 \times 10^6$ cMSC, hMSC, or mMSC were injected into the left ventricle (coordinate values SJL/JCrHsd: rostrocaudal 0 mm, lateral 2.2 mm, dorsoventral 1.7 mm; C57BL/6N: rostrocaudal − 0.2 mm, lateral 2.2 mm, dorsoventral 1.0 mm).

## Histology and Immunohistochemistry

The cerebrum was removed immediately after perfusion and fixed in 10% formalin for 24 h, embedded in paraffin wax, and processed for hematoxylin and eosin (HE) staining and immunohistochemistry.

Immunohistochemistry was performed with a panel of commercially available antibodies (summarized in Table 2) as previously described (Hansmann et al. 2012; Heinrich et al. 2015; Ulrich et al. 2008) using the avidin-biotin-peroxidase complex (ABC) method (Vector Laboratories, Burlingame, CA, USA). Briefly, 2–3-µm-thick sections were deparaffinized, rehydrated through a graded series of alcohols, and treated with 0.5% $H_2O_2$ to block endogenous peroxidase. Pretreatment was applied where applicable (Table 2). After blocking of non-specific reactions with goat serum, sections were incubated with either rat monoclonal antibodies, mouse monoclonal antibodies, or rabbit polyclonal antibodies. The EnVision System HRP (DAB, Dako, Hamburg, Germany) was used for anti-np-NF, anti-vimentin, and anti-human CD44 antibodies. For negative controls, primary antibodies were replaced by an appropriate amount of either rabbit-serum for polyclonal Abs (R4505; Sigma-Aldrich, Taufkirchen, Germany), mouse-serum IgG1 (CBL600; Chemicon, Hofheim/Taunus, Germany), ascites fluid (CI8100; Cedarlane, Burlington, Canada), or rat-serum (MCA1124R; R9759; Sigma-Aldrich, Taufkirchen, Germany) for monoclonal Abs. Antibody binding was visualized using 3,3-diaminobenzidine-tetrahydrochloride (DAB) and nuclei were counterstained with Mayer's hemalaun.

An immunohistochemical double labeling for the identification of proliferating cells was performed using a polyclonal rabbit anti-Ki67 (1:50; DCS innovative Diagnostic-Systems, Herford, Germany) antibody. Immunoreactivity was visualized using the anti-rabbit EnVision System-HRP (Dako, Hamburg, Germany) and DAB.

MSC were identified using anti-CD44 (1:100; AbD Serotec, Puchheim, Germany) as well as anti-vimentin (1:100; Dako Cytomation, Hamburg, Germany) antibodies. T lymphocytes were labeled using anti-CD3 (1:250; Bio Rad, Munich, Germany), B lymphocytes using anti-CD45R (1:1000; BD Bioscience, Heidelberg, Germany), microglia/macrophages using anti-CD107b (1:200; AbD Serotec, Puchheim, Germany), and astrocytes using anti-GFAP (1:500; Abcam, Cambridge, UK) antibodies. The visualization of the immunoreactivity was performed using biotinylated anti-rat immunoglobulins (Vector Laboratories, Burlingame, CA, USA), anti-goat immunoglobulins (Vector Laboratories, Burlingame, CA, USA), or the anti-mouse EnVision System-HRP (Dako, Hamburg, Germany) followed by Histogreen (LINARIS Biologische Produkte GmbH, Dossenheim, Germany) for rat, goat, and mouse originating primary antibodies, respectively. Immuno-positive cells were semi-quantitatively evaluated within the cell cluster and the surrounding brain parenchyma. The following scoring system was used: –, no; +, 0–20%; ++, 20–50%; +++, 50–80%, and ++++, > 80% of immuno-positive cells. Apoptotic cell death of transplanted MSC was quantified by counting caspase 3-labeled cells in a total of 200 cells within cell clusters and results were given as percentages.

**Table 2** Antibodies, suppliers, catalog numbers, sources, clonalities, pretreatments, dilution, and negative controls for immunohistochemical analysis

| Primary antibody | Supplier | Catalog number/RRID | Source and clonality | Pretreatment | Dilution | Negative control |
|---|---|---|---|---|---|---|
| CD44 | AbDSerotec‡ | MCA1041GA/AB_2074682 | Rat MC | Citrate buffer (pH 6.0) MW (800W) | 1:100 | Rat IgG2a, Serotec MCA1124R |
| CD44 | DakoCytomation** | M7082/AB_2076596 | Mouse MC | Citrate buffer (pH 6.0) MW (800W) | 1:100 | Balb/c, Cedarlane Cl8100 |
| Vimentin | DakoCytomation** | M0725/AB_10013485 | Mouse MC | – | 1:100 | Balb/c, Cedarlane Cl8100 |
| GFAP | DakoCytomation** | Z0334/AB_10013382 | Rabbit PC | – | 1:1000 | Rabbit serum, Sigma R4505 |
| GFAP | Abcam☯ | ab53554/AB_880202 | Goat PC | Citrate buffer (pH 6.0) MW (800W) | 1:500 | Goat serum, Sigma, I9140 |
| np-NF | Covance*** | SMI311R/AB_509992 | Mouse MC | Citrate buffer (pH 6.0) MW (800W) | 1:30000 | Mouse IgG1, Chemicon CBL600 |
| Cytokeratin | DakoCytomation** | M3515/AB_2132885 | Mouse MC | – | 1:500 | Balb/c, Cedarlane Cl8100 |
| NG2 | Chemicon* | AB5320/AB_91789 | Rabbit PC | Citrate buffer (pH 6.0) MW (800W) | 1:200 | Rabbit serum, Sigma R4505 |
| CNPase | Merck Millipore**** | MAB326/AB_2082608 | Mouse MC | Citrate buffer (pH 6.0) MW (800W) | 1:100 | Mouse IgG1, Chemicon CBL600 |
| MBP | Chemicon* | AB980/AB_92396 | Rabbit PC | – | 1:800 | Rabbit serum, Sigma R4505 |
| PECAM 1 | Acris antibodies♠ | AP15436PUM/AB_11149881 | Rabbit PC | Citrate buffer (pH 6.0) MW (800W) | 1:50 | Rabbit serum, Sigma R4505 |
| Caspase 3 | Cell signaling♦ | #9661/AB_2341188 | Rabbit PC | Citrate buffer (pH 6.0) MW (800W) | 1:200 | Rabbit serum, Sigma R4505 |
| Ki67 | DCS Innovative Diagnostik-Systeme♣ | Ki681R06/AB_2722785 | Rabbit MC | Citrate buffer (pH 6.0) MW (800W) | 1:400 | Rabbit serum, Sigma R4505 |
| CD3 | DakoCytomation** | A0452/AB_2335677 | Rabbit PC | Citrate buffer (pH 6.0) MW (800W) | 1:1000 | Rabbit serum, Sigma R4505 |
| CD3 | Bio Rad❖ | MCA1477/AB_321245 | Rat MC | Citrate buffer (pH 6.0) MW (800W) | 1:250 | Rat serum, Sigma |
| CD107b | AbD Serotec‡ | MCA2293/AB_2249788 | Rat MC | Citrate buffer (pH 6.0) MW (800W) | 1:200 | Rat serum, Sigma R9759 |
| CD45R | BDBioscience† | 553085/AB_394615 | Rat MC | Citrate buffer (pH 6.0) MW (800W) | 1:1000 | Rat serum, Sigma R9759 |

*CD* cluster of differentiation, *GFAP* glial fibrillary acidic protein, *MC* monoclonal, *MBP* myelin basic protein, *MW* microwave. *np-NF* non-phosphorylated neurofilaments, *PC* polyclonal

*Hofheim/Taunus, Germany

**Hamburg, Germany

☯ Cambridge, UK

***London, UK

****Darmstadt, Germany

† Heidelberg, Germany

‡ Puchheim, Germany

♠ Herford, Germany

♦ Leiden, Netherlands

♣ Hamburg, Germany

❖ Munich, Germany

## Results

### Isolation and Characterization of MSC In Vitro

cMSCs were adherent to plastic, grew in a monolayer, and showed a spindle-shaped morphology during in vitro culture. Cultivation of cMSC in differentiation media resulted in adipogenic, osteogenic, and chondrogenic differentiation of cMSC in accordance with previous publications (Guercio et al. 2013; Han et al. 2012; Reich et al. 2012).

Phenotypical characterization of cMSC using flow cytometry revealed a strong expression of CD44, CD90, CD29, and MHC I in more than 95% of the cells while less than 2% of the cells were positive for CD45.

Human MSC expressed CD90, CD73, CD105, and CD49d as described in Nessler et al. (2013) and Salinas Tejedor et al. (2015). RFP-labeled mMSC expressed CD44 and Sca-1 as described in detail by Salinas Tejedor et al. (2015).

### In Vivo Behavior of MSC at 7 Days Post Transplantation

Mice intraventricularly transplanted with cMSC or hMSC showed up to two, round to oval cell clusters within the ventricular system. Cell clusters were larger at 7 dpt compared to 49 dpt; no hMSC-containing cell clusters were detected at 49 dpt (Fig. 1). The central layer of cMSC and hMSC clusters consisted of medium-sized polygonal cells with distinct cell borders, a moderate amount of pale eosinophilic cytoplasm, and elongated nuclei (Fig. 2a, b). These cells showed a strong immunoreaction for CD44 (Fig. 2c, d). Only few cells expressed vimentin in the center of cMSC clusters (Fig. 2e) while the number of vimentin-expressing cells was higher in hMSC clusters (Fig. 2f). The center of cMSC clusters was surrounded by a peripheral layer consisting of spindle-shaped cells with indistinct cell borders, a moderate amount of pale eosinophilic cytoplasm, and elongated nuclei (Fig. 2a, arrows), showing many cells positive for CD44 (Fig. 2c) and vimentin (Fig. 2e). Cell clusters formed by both cMSC and hMSC were surrounded and partly infiltrated by inflammatory cells consisting of moderate numbers of CD3-positive T lymphocytes (Fig. 3a, b) as well as low numbers of CD107b-positive microglia/macrophages and CD45R-positive B lymphocytes (Table 3). Inflammatory cells were located perivascularly and within the parenchyma (Table 3). In the vicinity of the cell clusters, low numbers of GFAP-positive cells and np-NF-labeled axons were detected (Table 3). To address the question whether transplanted MSC underwent differentiation in vivo, immunohistochemistry targeting GFAP (astroglial differentiation), pan cytokeratin (epithelial differentiation), NG2, CNPase, and MBP (oligodendroglial differentiation) as well as PECAM1 (endothelial differentiation) was performed (Table 3). Neither transplanted cMSCs nor hMSCs were positive for one of these markers indicating a lack of MSC differentiation in vivo compared to reported in vitro *transdifferentiation properties*.

The question whether MSCs gained in number by proliferation or are reduced by apoptosis was addressed by immunohistochemical double labeling using Ki67 for identification of cell proliferation and caspase 3 for identification of apoptosis. Moderate numbers of Ki67-labeled cells were detected in the periphery of cMSC and hMSC clusters (Fig. 3c, d). Furthermore, a low percentage of caspase 3-labeled cells was detected in canine (0.5–1.5%) and human (1–7%) cell clusters. However, CD44-positive cells were negative for caspase 3 (Fig. 3e, f).

Colocalization for Ki67 with the MSC markers CD44 or vimentin (Fig. 4a, b) was not visible, while double labeling for

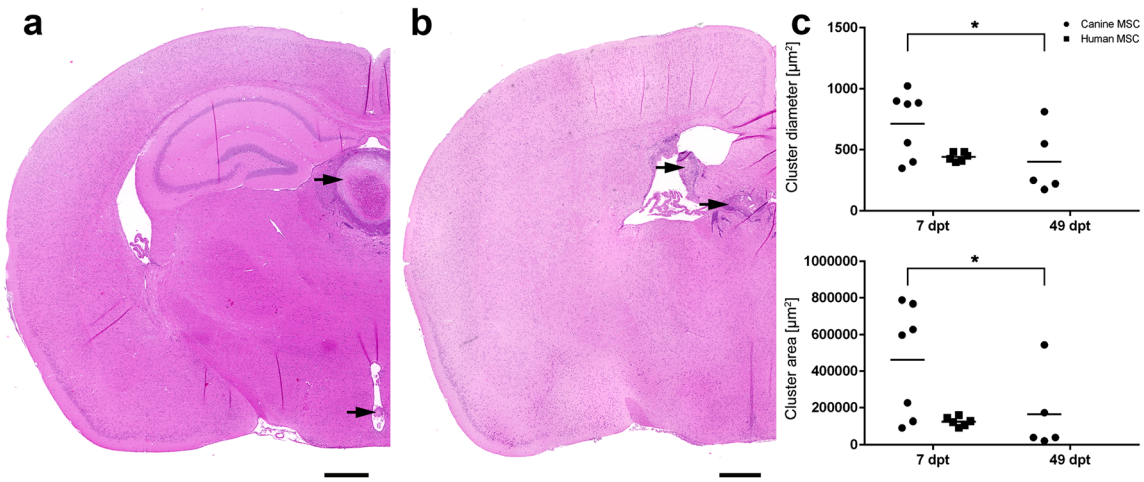


**Fig. 1** Transplanted canine (**a**) and human (**b**) mesenchymal stem cells (MSC) form intraventricular cell clusters (arrows) at 7 dpt. Scatter dot plots show diameter and area of detected cell clusters at 7 and 49 days post transplantation (**c**). At 7 dpt, no significant difference between human and canine MSC with respect to size and diameter was detected. Both diameter and cluster area were significantly larger in cMSC-transplanted animals at 7 dpt compared to 49 dpt. Bars = 500 µm

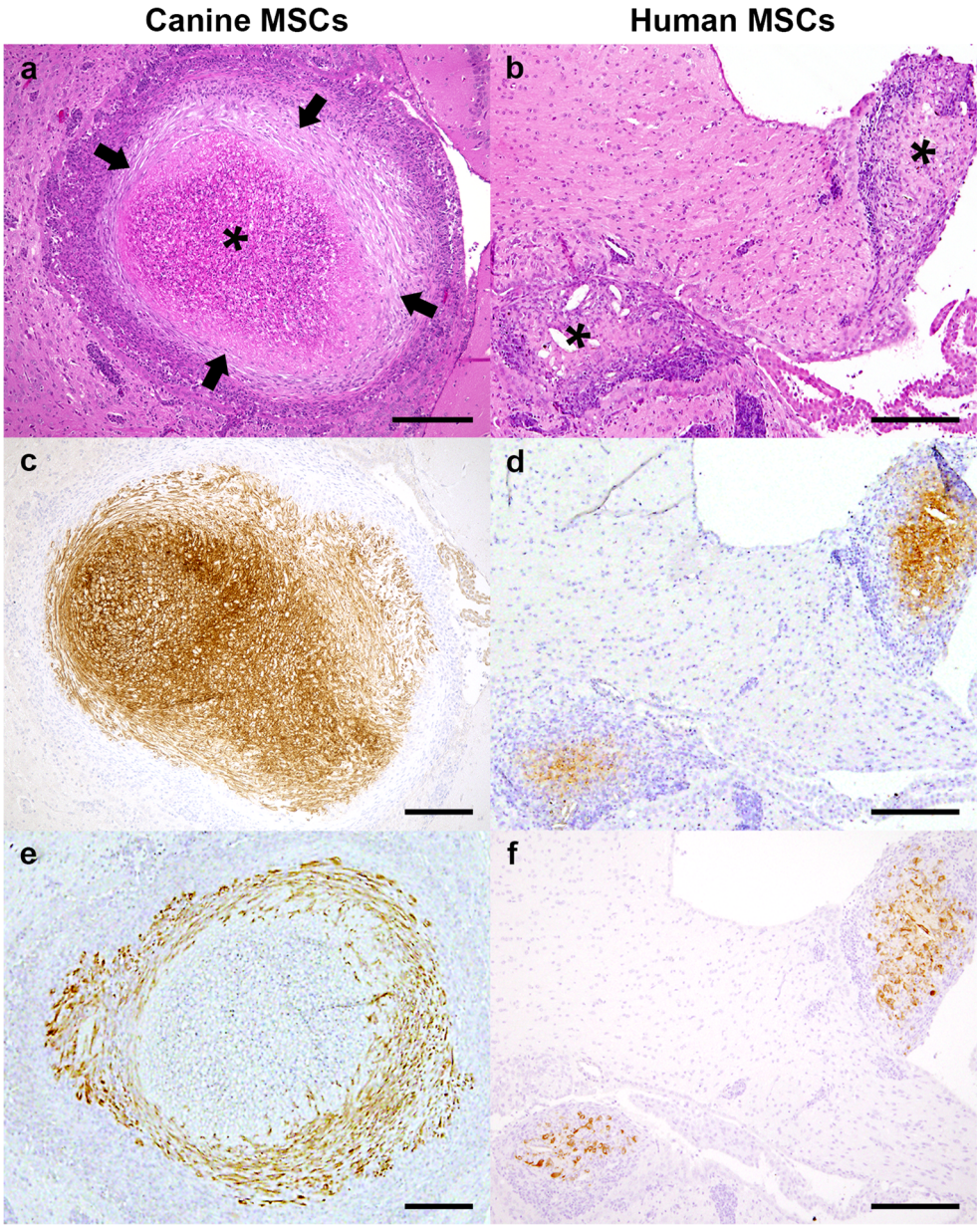


**Fig. 2** Cell clusters of canine MSC (cMSC) and human MSC (hMSC) at 7 days post xenogeneic transplantation into the ventricular system. **a** cMSC clusters consist of two layers, a central (asterisk) surround by a peripheral (arrows). **b** hMSC clusters displayed a more homogenous appearance lacking distinct layers (asterisks). **c**, **d** Immunohistochemistry targeting strongly CD44-labeled cMSC located in the central layer as well as hMSC. **e** The peripheral layer of cMSC clusters consists of spindle-shaped cells labeled by anti-vimentin antibodies. **f** hMSC cell clusters showed multifocal vimentin-expressing cells. Bars = 200 μm

Ki67 and GFAP (Fig. 4c), CD3 (Fig. 4d), CD45R (Fig. 4e), and CD107b (Fig. 4f) was observed. These findings indicate that MSC did not proliferate in vivo while adjacent immune cells increased in number by proliferation supporting the hypothesis of an immune-mediated graft rejection.

## In Vivo Behavior of MSC at 49 Days Post Transplantation

At 49 dpt, remnants of cell clusters were detected in cMSC-transplanted mice while no cell clusters were observed in hMSC-transplanted animals. Cell clusters were poorly cellular, consisted of a pale eosinophilic, homogenous extracellular matrix (Fig. 5a) and were smaller at 49 dpt compared to 7 dpt (Fig. 1). Cells within cell clusters were negative for CD44 (Fig. 5b) but positive for CD3 (Fig. 5c), CD107b, or CD45R. In the vicinity of the cell clusters, a moderate number of GFAP-positive cells (Fig. 5d) and low numbers of CD3-positive cells as well as np-NF-labeled axons and few caspase 3-labeled cells were detected (Table 3).

## Impact of MSC Origin upon the Observed Immune Reaction

Since xenogeneic intraventricular cMSC and hMSC transplantation in SJL mice was associated with an inflammatory cell reaction, additional experiments investigating the underlying pathogenesis were performed. Experimental setting included an intraventricular transplantation of C57BL/6N-derived, RFP-labeled MSC into C57BL/6N mice (syngeneic

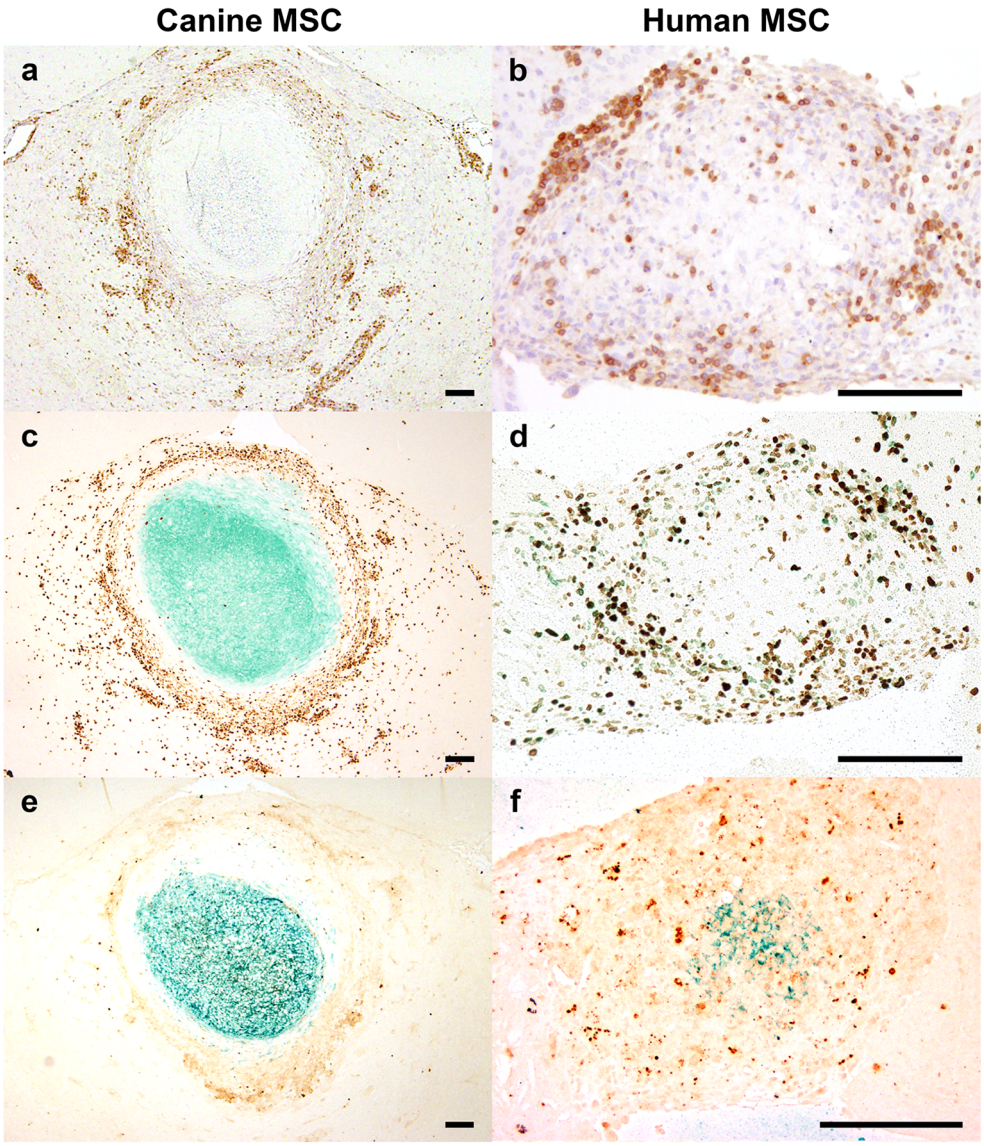


**Fig. 3** Immunophenotyping of inflammatory cells at 7 days post xenogeneic transplantation of canine MSC (cMSC) and human MSC (hMSC) into the ventricular system. **a** cMSC-transplanted mice showed in the periphery of cMSC cell clusters as well as in their vicinity a mild to moderate number of CD3 positive T lymphocytes. **b** hMSC cell clusters showed an infiltration of CD3-positive T lymphocytes. Additionally, CD3-positive cells were detected in the surrounding parenchyma as well as perivascularly. **c**, **d** Immunohistochemical double labeling showed many CD44-positive MSC (green) and moderate numbers of Ki67-labeled cells (brown). No cells positive for CD44 and Ki67 were detected. **e** Low numbers of caspase 3-labeled cells were detected at the periphery of cMSC cell clusters (green). Interestingly, cMSCs were negative for caspase 3. **f** Within hMSC clusters, low numbers of caspase 3-positive cells (brown) were detected. Cells positive for CD44 and caspase 3 were not observed. Bars = 100 μm

transplantation). mMSC formed intraventricular cell clusters with a morphology similar to that observed following cMSC and hMSC transplantation (Fig. 6a, b). Interestingly, in mMSC-transplanted animals, cell clusters were not associated with an inflammatory cell reaction (Fig. 6c, d), indicating that the inflammatory cells observed following xenogeneic cMSC and hMSC transplantation are due to a host-versus-graft reaction.

## Discussion

The aim of this study was to comparatively investigate the in vivo behavior of cMSC, hMSC, and mMSC following intraventricular transplantation in immunocompetent mice. Special emphasis was given to survival of transplanted MSC, their capacity to differentiate and/or integrate into the host tissue, and their interaction with the immune system.

### In Vivo Behavior of MSC at 7 Days Post Transplantation

Mesenchymal stem cell properties of transplanted cells, according to the criteria of the International Society for Cell Therapy (Dominici et al. 2006), were confirmed in vitro previous to transplantation. Following xenogeneic (cMSC, hMSC) as well as syngeneic (mMSC) transplantation of MSC into the ventricular system, a similar formation of intraventricular cell clusters was detected. The detection of MSC clusters within the ventricular system represents a rather unexpected finding following MSC transplantation. The observed cell cluster formation may be promoted by a strong cell-cell contact during in vitro culture prior to transplantation.

**Table 3** Immunohistochemical characterization of canine MSC (cMSC) and human MSC (hMSC) clusters within the ventricular system of mice. Scoring system for the semi-quantitative evaluation was determined as follows: –, no; +, 0–20%; ++, 20–50%; +++, 50–80%; and ++++, > 80% of immuno-positive cells. *np-NF* non-phosphorylated neurofilaments, *n.d.* non-determined

| Marker | cMSC clusters at 7dpt | | | hMSC clusters at 7dpt | | cMSC clusters at 49dpt | |
|---|---|---|---|---|---|---|---|
| | Central layer | Peripheral layer | Parenchyma in cluster vicinity | Central layer | Parenchyma in cluster vicinity | Central layer | Parenchyma in cluster vicinity |
| CD44 | ++++ | ++ | – | – | – | – | – |
| Vimentin | – | ++++ | – | – | – | – | – |
| GFAP | – | – | + | – | +++ | – | ++ |
| np-NF | – | – | + | – | + | – | + |
| Cytokeratin | – | – | – | + | – | n.d. | n.d. |
| NG2 | – | – | + | + | + | n.d. | n.d. |
| CNPase | – | – | + | – | – | n.d. | n.d. |
| PECAM 1 | – | – | + | – | + | n.d. | n.d. |
| Caspase 3 | + | – | + | + | – | – | + |
| Ki67 | – | + | ++ | ++ | ++ | ++ | +++ |
| CD3 | – | – | ++ | +++ | ++ | ++ | +++ |
| CD107b | – | – | + | ++ | – | + | + |
| CD45R | – | – | + | + | – | + | + |

Other mechanisms contributing to or promoting this behavior may be the turbidity of the cerebrospinal fluid (CSF) as well as exogenous factors solved in CSF or secreted by the local environment. Cell cluster (spheroid) formation can be induced under experimental conditions in tissue culture since 3D cell spheroids display more in vivo-*like* properties than 2D cell monolayers (Haeger et al. 2011). In addition, for chondrogenesis, MSCs are cultured in pellets to mimic the anaerobic conditions within cartilage and cluster formation of tumor cells represents a mechanism for the avoidance of apoptosis (Lee et al. 2009; Santini et al. 2000).

Cell cluster morphology varied between both MSC types in so far as cMSC clusters consisted of two layers (central, peripheral) compared to hMSC, which showed a more homogenous distribution of cell populations lacking an organization in distinct layers. However, the different morphological arrangement of cell clusters was not associated with altered effects of the transplanted cells. The central area in both species was characterized by medium-sized polygonal cells with a strong immunopositivity for CD44. CD44 serves as a suitable MSC tracking and identification marker since this molecule is strongly expressed by cMSC and hMSC (Mimeault et al. 2007; Salinas Tejedor et al. 2015; Screven et al. 2014) and no resident endogenous cells in the murine CNS were labeled by this antibody. MSC origin was further substantiated by the detection of vimentin either distributed in the middle area of cMSC clusters or multifocal within the center of hMSC clusters. This is consistent with previous publications describing vimentin expression by MSC (Romanov et al. 2005). Transplanted MSC did not show any differentiation into brain-resident cell lineages in vivo (Table 3). To address the question whether the number of MSC was reduced over time by a lack of proliferation, an increased rate of apoptosis, or a combination of these, immunohistochemical double labeling for Ki67 (cell proliferation) and CD44 (MSC) as well as caspase 3 (apoptosis marker) and MSC was performed. Ki67-labeled cells were detected within the cell clusters as well as in their close vicinity. However, no MSCs were positive for Ki67 indicating that the cells themselves and/or the surrounding environment were insufficient to establish cell proliferation in vivo. Instead, surrounding lymphocytes as well as astrocytes were labeled by Ki67 supporting the hypothesis of a lymphocyte-mediated graft rejection. In addition, a low number of caspase 3-positive cells were detected within cell clusters and in close vicinity but no cells labeled for CD44 and caspase 3 were detected. This finding indicates that the observed reduction/lack of transplanted MSC at 49 dpt is not related to a primary increased rate of apoptosis but may result from an anti-graft immune response supported by microglia/macrophage-mediated phagocytosis and removal.

Surrounding hMSC clusters, a mild astrogliosis was detected indicating a demarcation of the transplanted cells. Activation of astrocytes represents a common mechanism which takes place following various triggers including tissue damage, infectious, and degenerative diseases (Sofroniew and Vinters 2010).

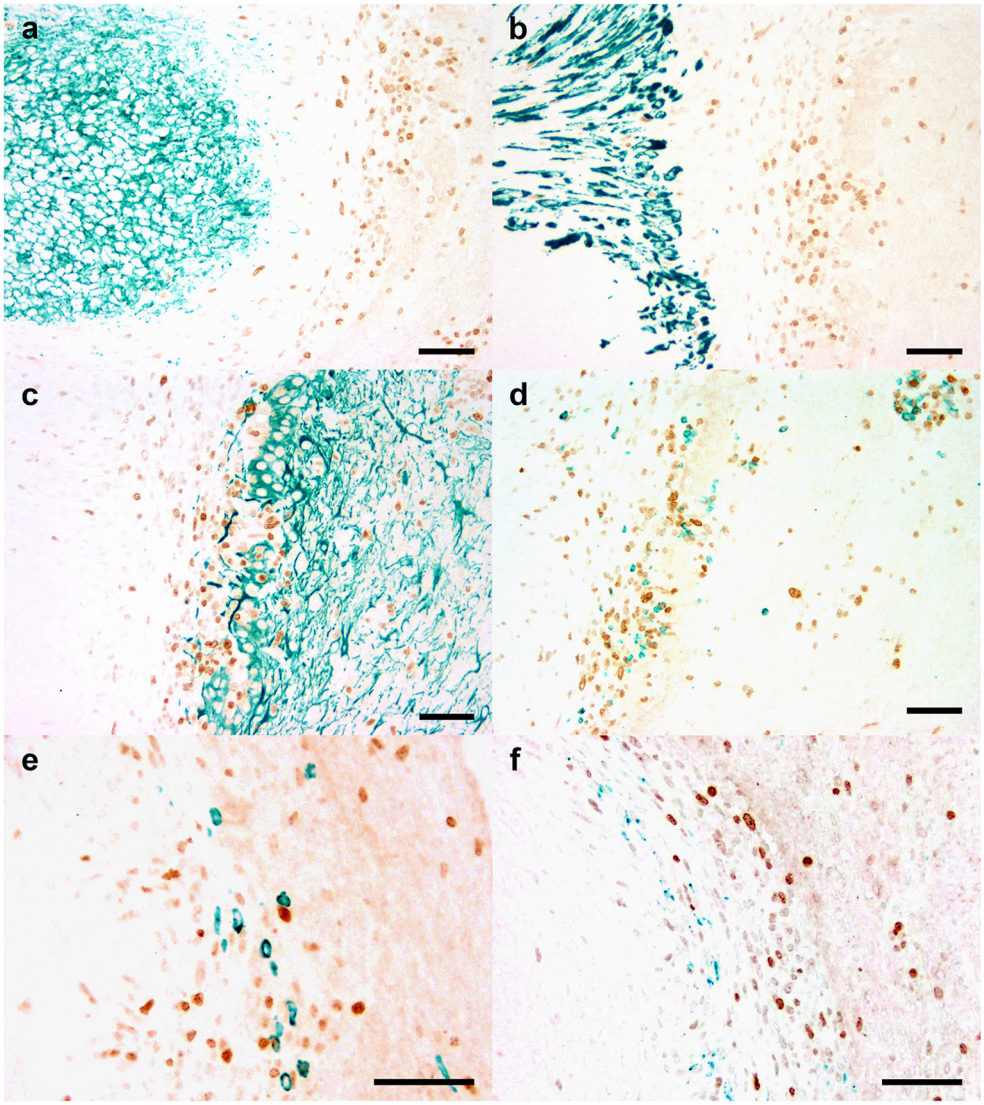


**Fig. 4** Immunophenotyping of proliferating cells at 7 days post canine MSC (cMSC) transplantation. Immunophenotyping of proliferating cells in and around clusters of cMSC was performed using immunohistochemical double labeling using Ki67 in combination with respective cell type markers. **a** Clusters in cMSC-transplanted mice showed a strong, centrally located reactivity for the MSC marker CD44 (green) but no colocalization with Ki67 (brown) was observed indicating a lack of cMSC proliferation in vivo. A colocalization for Ki67 (brown) and vimentin (green, **b**), GFAP (green, **c**), CD3 (green, **d**), CD45R (green, **e**), and CD107b (green, **f**) was detected. Bars = 50 μm

## In Vivo Behavior of MSC at 49 Days Post Transplantation

The second time point was chosen to investigate long-term survival, integration, and effects of MSC on host tissue as different studies showed a good short time survival of transplanted cells (Gordon et al. 2010; Kang et al. 2012; Salinas Tejedor et al. 2015; van Velthoven et al. 2010). A previous publication indicated that long-term engraftment and cell survival should not be investigated earlier than 4 weeks' post transplantation since in this timeframe, acute and delayed immune rejections are initiated (Anderson et al. 2011). Interestingly, at 49 dpt in cMSC-transplanted mice, remnants of cell clusters consisting of a poorly cellular aggregation of extracellular matrix were detected while no cell clusters were found in hMSC-transplanted mice. The detection of similar masses was described following intracerebroventricular transplantation of bone marrow-derived MSC in experimental autoimmune encephalomyelitis (EAE; Grigoriadis et al. 2011). Those masses in close vicinity to the ventricular system showed an increased amount of extracellular matrix surrounding MSC. In this study, the number of transplanted cells, the density of grafted cells following periventricular migration, and the presence of an EAE-associated inflammatory reaction were identified to be key factors for the mass formation of bone marrow-derived MSC (Grigoriadis et al. 2011). A further study showed a mass formation consisting of an amorphous, osteocalcin-positive material and MSC within infarcted hearts following intravenous MSC transplantation (Breitbach et al. 2007). However, in the present study, presumptive MSC clusters were negative for CD44 as well as vimentin. The lack of CD44-positive cells may result from the fact that the transplanted MSC reached their end of life since they failed to proliferate in vivo and did not integrate into the host tissue as indicated at 7 dpt. Since MSCs were negative for caspase 3, the observed reduction of

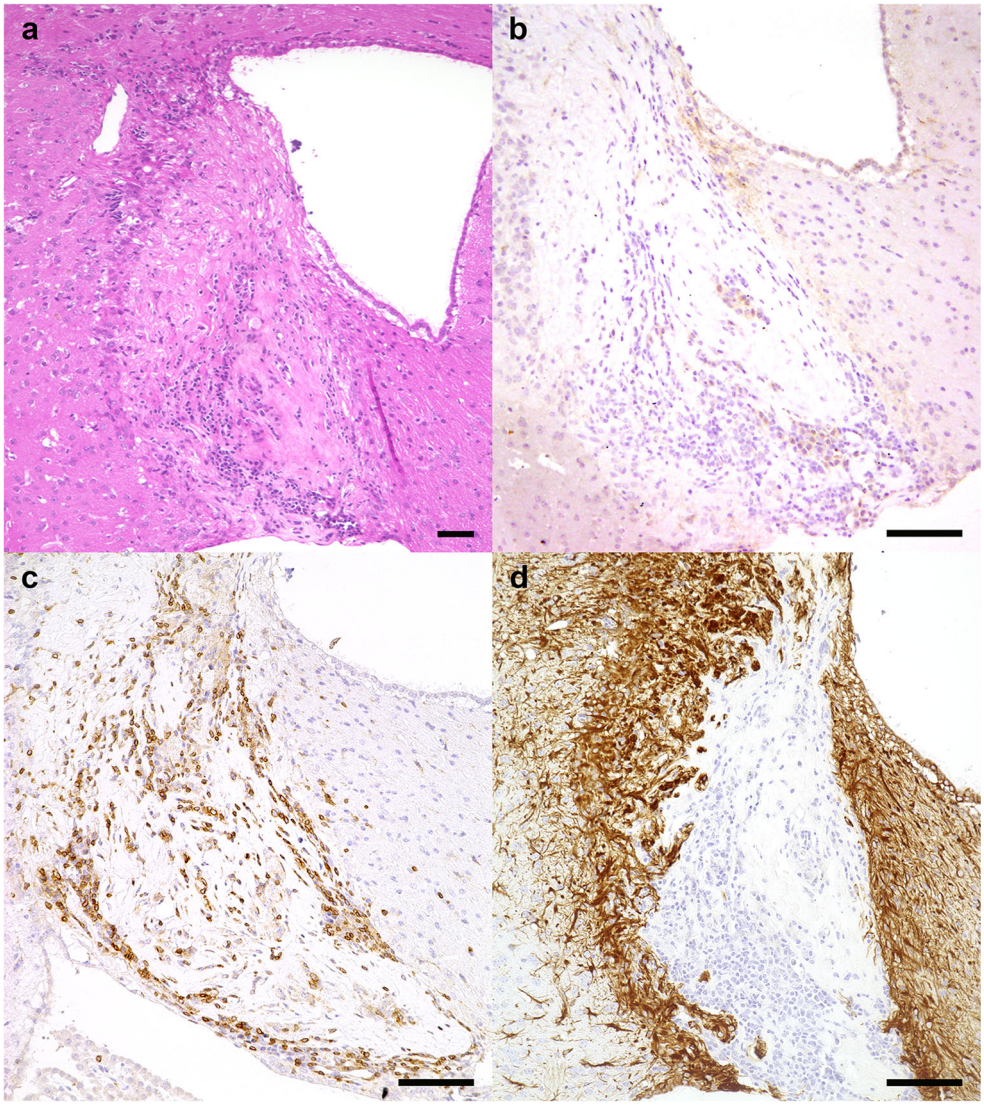


**Fig. 5** Characterization of canine MSC (cMSC) at 49 days post xenogeneic transplantation into the ventricular system. **a** Cell clusters were poorly cellular consisting of an accumulation of extracellular matrix. **b** Within clusters, no CD44-positive cells were detected using immunohistochemistry. **c** Immunohistochemistry targeting CD3 revealed moderate numbers of positive T lymphocytes within the clusters. **d** Glial fibrillary acidic protein (GFAP) was visualized using immunohistochemistry highlighting a moderate to severe number of GFAP-positive astrocytes surrounding the clusters. Bars = 100 μm

cluster size and diameter may be caused by phagocytosis of transplanted MSC by microglia/macrophages. Another factor which cannot be completely excluded is that cMSC lost their CD44 expression during 49 days in vivo but this is unlikely since cells within the clusters did not show an MSC-like morphology. Other factors contributing to the loss of MSC may be a hostile environment generated by an astrogliosis surrounding MSC clusters in concert with an aggregation/infiltration of inflammatory cells.

## Interaction of MSC with the Immune System

Rejection and limited survival following transplantation of neural stem cells as well as MSC have been described in previous studies (von Bahr et al. 2012; Weinger et al. 2012). However, MSC may mediate their effects by a "hit and run" mechanism and the lack of engraftment associated with a limited survival of MSC bears the advantage of a limited risk for long-term MSC therapy (von Bahr et al. 2012). Mechanisms leading to graft cell destruction were related to the recognition of surface antigens (MHC molecules) by the innate immune system leading to an activation of T lymphocytes recognizing graft epitopes. The infiltration of cMSC and hMSC clusters by T lymphocytes in the present study represents an unexpected finding since MSCs are considered to be immune privileged or of low immunogenicity (Le Blanc et al. 2003). To address the question whether the observed T lymphocytes are directly related to the transplanted MSC, an additional experiment was performed. In this study, C57BL/6N mice received an intraventricular transplantation of mMSC (syngeneic transplantation). Similar to the observations obtained following cMSC and hMSC transplantation, mMSC formed intraventricular cell clusters, but an associated inflammatory cell reaction was not observed (Fig. 6). It seems likely that the T lymphocyte-dominated immune response surrounding and/or within the cell clusters is triggered by the transplanted MSC.

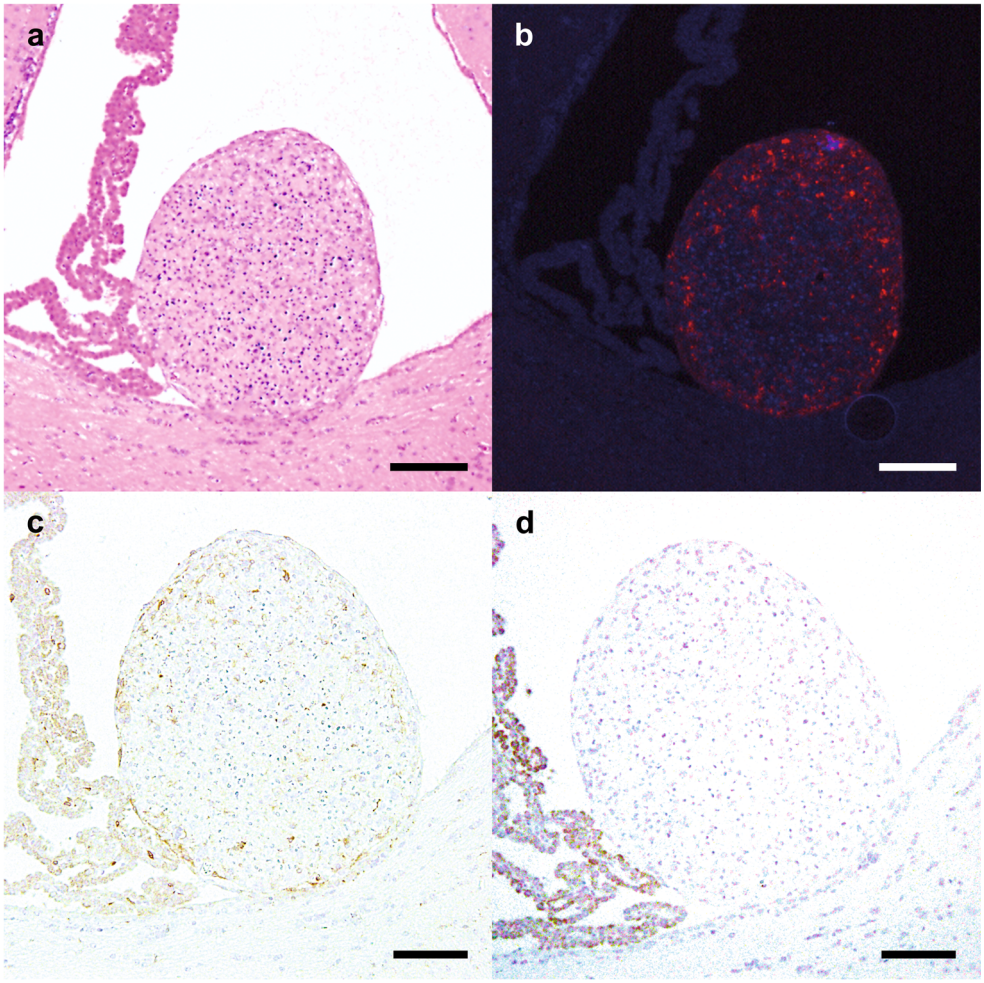


**Fig. 6** Characterization of murine MSC (mMSC) at 7 days post syngeneic transplantation into the ventricular system. **a** Intraventricularly located round to oval cell clusters formed by murine MSC (mMSC) in direct contact with ependymal cells. In the vicinity of cell clusters, no inflammatory cell reaction can be observed (HE). **b** Immunofluorescence showing RFP-labeled mMSC (red) within intraventricular cell clusters. Nuclei were stained using bisbenzimide (blue). **c** Immunohistochemistry targeting CD3 revealed low numbers of T lymphocytes within the clusters while no positive cells were seen in the vicinity of the clusters. **d** CD45R-positive B lymphocytes were neither detected within cell clusters nor within the surrounding parenchyma. Bars = 100 μm

This assumption is supported by detection of MHC class I expression on transplanted MSC. Moreover, foreign MHC I molecules trigger an activation and proliferation of host T lymphocytes leading finally to transplant destruction (Hoogduijn et al. 2010; Ingulli 2010). The lack of CD44-positive cells in cMSC- and hMSC-transplanted mice at 49 dpt in combination with an increased number of T lymphocytes indicates that MSCs are not immune privileged but may induce a T lymphocyte-mediated immune response.

## Conclusion

MSC of canine, human, and murine origin similarly formed intraventricular cell clusters following transplantation. The survival time of MSC following transplantation into the ventricular system of healthy mice was limited since transplanted MSC neither proliferated nor underwent further differentiation. Xenogeneic transplantation of canine and human MSC was followed by a T lymphocyte-dominated anti-graft reaction which was not observed following syngeneic MSC transplantation indicating a better in vivo survival of syngeneically transplanted MSC. However, future studies will show whether syngeneically or xenogeneically transplanted MSCs exert better therapeutic effects in animals with CNS disease.

**Acknowledgments** The authors thank Caroline Schütz, Petra Grünig, Kerstin Schöne, Kerstin Rohn, Regina Carlson, Danuta Waschke, and Bettina Buck for excellent technical assistance. The authors also thank PD Dr. Manuela Gernert, Department of Pharmacology, University of Veterinary Medicine, Hannover, Germany, and Alexander Klein, Department of Neuroanatomy, Medical School Hannover, Germany, for scientific advice. Parts of the data were published in the thesis of Nicole Jungwirth (Deutsche Veterinärmedizinische Gesellschaft, 2016).

**Funding Information** W. Baumgärtner, M. Stangel, and A. Tipold were supported by the German Research Foundation (Deutsche Forschungsgemeinschaft, Forschergruppe 1103, BA 815/14-1, STA 518/4-1, TI 309/4-2). This study was in part supported by the Niedersachsen-Research Network on Neuroinfectiology (N-RENNT) of the Ministry of Science and Culture of Lower Saxony, Germany.

## Compliance with Ethical Standards

Human bone marrow-derived mesenchymal stem cells (hMSCs) were isolated from a healthy, female donor after consent of the ethics committee of Hannover Medical School. Animal experiments were conducted in accordance with the German Animal Welfare Law and all experiments were

approved by the local authorities (Niedersächsisches Landesamt für Verbraucherschutz und Lebensmittelsicherheit (LAVES), Oldenburg, Germany, permission numbers: 33.12-42502-04-13/1071 and 33.9-42502-05-13A302; Landesamt für Natur, Umwelt und Verbraucherschutz (LANUV), Recklinghausen, Germany, permission number: 501/A80).

## References


Anderson AJ, Haus DL, Hooshmand MJ, Perez H, Sontag CJ, Cummings BJ (2011) Achieving stable human stem cell engraftment and survival in the CNS: is the future of regenerative medicine immunodeficient? Regen Med 6:367–406

Barry FP, Murphy JM (2004) Mesenchymal stem cells: clinical applications and biological characterization. Int J Biochem Cell Biol 36: 568–584

Bernardo ME, Fibbe WE (2013) Mesenchymal stromal cells: sensors and switchers of inflammation. Cell Stem Cell 13:392–402

Breitbach M, Bostani T, Roell W, Xia Y, Dewald O, Nygren JM, Fries JW, Tiemann K, Bohlen H, Hescheler J, Welz A, Bloch W, Jacobsen SE, Fleischmann BK (2007) Potential risks of bone marrow cell transplantation into infarcted hearts. Blood 110:1362–1369

de Bakker E, Van Ryssen B, De Schauwer C, Meyer E (2013) Canine mesenchymal stem cells: state of the art, perspectives as therapy for dogs and as a model for man. Vet Q 33:225–233

Dominici M, Le Blanc K, Mueller I, Slaper-Cortenbach I, Marini F, Krause D, Deans R, Keating A, Prockop D, Horwitz E (2006) Minimal criteria for defining multipotent mesenchymal stromal cells. The International Society for Cellular Therapy position statement. Cytotherapy 8:315–317

Edamura K, Kuriyama K, Kato K, Nakano R, Teshima K, Asano K, Sato T, Tanaka S (2012) Proliferation capacity, neuronal differentiation potency and microstructures after the differentiation of canine bone marrow stromal cells into neurons. J Vet Med Sci 74:923–927

Fortier LA, Travis AJ (2011) Stem cells in veterinary medicine. Stem Cell Res Ther 2:9

Friedenstein AJ, Piatetzky S II, Petrakova KV (1966) Osteogenesis in transplants of bone marrow cells. J Embryol Exp Morphol 16: 381–390

Gordon D, Pavlovska G, Uney JB, Wraith DC, Scolding NJ (2010) Human mesenchymal stem cells infiltrate the spinal cord, reduce demyelination, and localize to white matter lesions in experimental autoimmune encephalomyelitis. J Neuropathol Exp Neurol 69: 1087–1095

Grigoriadis N, Lourbopoulos A, Lagoudaki R, Frischer JM, Polyzoidou E, Touloumi O, Simeonidou C, Deretzi G, Kountouras J, Spandou E, Kotta K, Karkavelas G, Tascos N, Lassmann H (2011) Variable behavior and complications of autologous bone marrow mesenchymal stem cells transplanted in experimental autoimmune encephalomyelitis. Exp Neurol 230:78–89

Guercio A, Di Bella S, Casella S, Di Marco P, Russo C, Piccione G (2013) Canine mesenchymal stem cells (MSCs): characterization in relation to donor age and adipose tissue-harvesting site. Cell Biol Int 37:789–798

Haeger JD, Hambruch N, Dilly M, Froehlich R, Pfarrer C (2011) Formation of bovine placental trophoblast spheroids. Cells Tissues Organs 193:274–284

Han SM, Lee HW, Bhang DH, Seo KW, Youn HY (2012) Canine mesenchymal stem cells are effectively labeled with silica nanoparticles and unambiguously visualized in highly autofluorescent tissues. BMC Vet Res 8:145

Hansmann F, Herder V, Kalkuhl A, Haist V, Zhang N, Schaudien D, Deschl U, Baumgärtner W, Ulrich R (2012) Matrix metalloproteinase-12 deficiency ameliorates the clinical course and demyelination in Theiler's murine encephalomyelitis. Acta Neuropathol 124:127–142

Harding J, Roberts RM, Mirochnitchenko O (2013) Large animal models for stem cell therapy. Stem Cell Res Ther 4:23

Heinrich F, Jungwirth N, Carlson R, Tipold A, Böer M, Scheibe T, Molnár V, von Dörnberg K, Spitzbarth I, Puff C, Wohlsein P, Baumgärtner W (2015) Immunophenotyping of immune cell populations in the raccoon (Procyon lotor). Vet Immunol Immunopathol 168:140–146

Herder V, Hansmann F, Stangel M, Schaudien D, Rohn K, Baumgärtner W, Beineke A (2012) Cuprizone inhibits demyelinating leukomyelitis by reducing immune responses without virus exacerbation in an infectious model of multiple sclerosis. J Neuroimmunol 244:84–93

Hernigou P (2015) Bone transplantation and tissue engineering, part IV. Mesenchymal stem cells: history in orthopedic surgery from Cohnheim and Goujon to the Nobel Prize of Yamanaka. Int Orthop 39:807–817

Hoogduijn MJ, Popp F, Verbeek R, Masoodi M, Nicolaou A, Baan C, Dahlke MH (2010) The immunomodulatory properties of mesenchymal stem cells and their use for immunotherapy. Int Immunopharmacol 10:1496–1500

Ingulli E (2010) Mechanism of cellular rejection in transplantation. Pediatr Nephrol 25:61–74

Jeffery ND, Smith PM, Lakatos A, Ibanez C, Ito D, Franklin RJ (2006) Clinical canine spinal cord injury provides an opportunity to examine the issues in translating laboratory techniques into practical therapy. Spinal Cord 44:584–593

Jung DI, Ha J, Kang BT, Kim JW, Quan FS, Lee JH, Woo EJ, Park HM (2009) A comparison of autologous and allogenic bone marrow-derived mesenchymal stem cell transplantation in canine spinal cord injury. J Neurol Sci 285:67–77

Kang ES, Ha KY, Kim YH (2012) Fate of transplanted bone marrow derived mesenchymal stem cells following spinal cord injury in rats by transplantation routes. J Korean Med Sci 27:586–593

Karp JM, Leng Teo GS (2009) Mesenchymal stem cell homing: the devil is in the details. Cell Stem Cell 4:206–216

Le Blanc K, Mougiakakos D (2012) Multipotent mesenchymal stromal cells and the innate immune system. Nat Rev Immunol 12:383–396

Le Blanc K, Tammik C, Rosendahl K, Zetterberg E, Ringden O (2003) HLA expression and immunologic properties of differentiated and undifferentiated mesenchymal stem cells. Exp Hematol 31:890–896

Lee RH, Pulin AA, Seo MJ, Kota DJ, Ylostalo J, Larson BL (2009) Intravenous hMSCs improve myocardial infarction in mice because cells embolized in lung are activated to secrete the anti-inflammatory protein TSG-6. Cell Stem Cell 5:54–63

Martinello T, Bronzini I, Maccatrozzo L, Mollo A, Sampaolesi M, Mascarello F, Decaminada M, Patruno M (2011) Canine adipose-derived-mesenchymal stem cells do not lose stem features after a long-term cryopreservation. Res Vet Sci 91:18–24

Mimeault M, Hauke R, Batra SK (2007) Stem cells: a revolution in therapeutics-recent advances in stem cell biology and their therapeutic applications in regenerative medicine and cancer therapies. Clin Pharmacol Ther 82:252–264

Nessler J, Benardais K, Gudi V, Hoffmann A, Salinas Tejedor L, Janssen S, Prajeeth CK, Baumgärtner W, Kavelaars A, Heijnen CJ, van Velthoven C, Hansmann F, Skripuletz T, Stangel M (2013) Effects of murine and human bone marrow-derived mesenchymal stem cells on cuprizone induced demyelination. PLoS One 8:e69795

Reich CM, Raabe O, Wenisch S, Bridger PS, Kramer M, Arnhold S (2012) Isolation, culture and chondrogenic differentiation of canine adipose tissue- and bone marrow-derived mesenchymal stem cells—a comparative study. Vet Res Commun 36:139–148

Romanov YA, Darevskaya AN, Merzlikina NV, Buravkova LB (2005) Mesenchymal stem cells from human bone marrow and adipose

tissue: isolation, characterization, and differentiation potentialities. Bull Exp Biol Med 140:138–143

Salinas Tejedor L, Berner G, Jacobsen K, Gudi V, Jungwirth N, Hansmann F, Gingele S, Prajeeth CK, Baumgärtner W, Hoffmann A, Skripuletz T, Stangel M (2015) Mesenchymal stem cells do not exert direct beneficial effects on CNS remyelination in the absence of the peripheral immune system. Brain Behav Immun 50:155–165

Santini MT, Rainaldi G, Indovina PL (2000) Apoptosis, cell adhesion and the extracellular matrix in the three-dimensional growth of multicellular tumor spheroids. Crit Rev Oncol Hematol 36:75–87

Screven R, Kenyon E, Myers MJ, Yancy HF, Skasko M, Boxer L, Bigley EC 3rd, Borjesson DL, Zhu M (2014) Immunophenotype and gene expression profile of mesenchymal stem cells derived from canine adipose tissue and bone marrow. Vet Immunol Immunopathol 161:21–31

Singer NG, Caplan AI (2011) Mesenchymal stem cells: mechanisms of inflammation. Annu Rev Pathol 6:457–478

Sofroniew MV, Vinters HV (2010) Astrocytes: biology and pathology. Acta Neuropathol 119:7–35

Spitzbarth I, Baumgärtner W, Beineke A (2012) The role of pro- and anti-inflammatory cytokines in the pathogenesis of spontaneous canine CNS diseases. Vet Immunol Immunopathol 147:6–24

Stein VM, Czub M, Hansen R, Leibold W, Moore PF, Zurbriggen A, Tipold A (2004) Characterization of canine microglial cells isolated ex vivo. Vet Immunol Immunopathol 99:73–85

Uccelli A, Moretta L, Pistoia V (2008) Mesenchymal stem cells in health and disease. Nat Rev Immunol 8:726–736

Ulrich R, Seeliger F, Kreutzer M, Germann PG, Baumgärtner W (2008) Limited remyelination in Theiler's murine encephalomyelitis due to insufficient oligodendroglial differentiation of nerve/glial antigen 2 (NG2)-positive putative oligodendroglial progenitor cells. Neuropathol Appl Neurobiol 34:603–620

van Velthoven CT, Kavelaars A, van Bel F, Heijnen CJ (2010) Nasal administration of stem cells: a promising novel route to treat neonatal ischemic brain damage. Pediatr Res 68:419–422

Vieira NM, Brandalise V, Zucconi E, Secco M, Strauss BE, Zatz M (2010). Isolation, characterization, and differentiation potential of canine adipose-derived stem cells. Cell Transplant 19:279–289

von Bahr L, Batsis I, Moll G, Hagg M, Szakos A, Sundberg B, Uzunel M, Ringden O, Le Blanc K (2012) Analysis of tissues following mesenchymal stromal cell therapy in humans indicates limited long-term engraftment and no ectopic tissue formation. Stem Cells 30:1575–1578

Weinger JG, Weist BM, Plaisted WC, Klaus SM, Walsh CM, Lane TE (2012) MHC mismatch results in neural progenitor cell rejection following spinal cord transplantation in a model of viral-induced demyelination. Stem Cells 30:2584–2595

Whitworth DJ, Banks TA (2014) Stem cell therapies for treating osteoarthritis: prescient or premature? Vet J 202:416–424

Woodbury D, Schwarz EJ, Prockop DJ, Black IB (2000) Adult rat and human bone marrow stromal cells differentiate into neurons. J Neurosci Res 61:364–370